

## **Robustness of Chimera states in Nonlocally Coupled Logistic Maps**

Pranneetha B<sup>1</sup> and Nita Parekh<sup>2</sup>

- <sup>1</sup> Centre for Computational Natural Science and Bio-informatics, IIIT Hyderabad.  
(E-mail: pranneetha.bellamkonda@students.iiit.ac.in)
- <sup>2</sup> Centre for Computational Natural Science and Bio-informatics, IIIT Hyderabad.  
(E-mail: nita@iiit.ac.in)

**Abstract:** In the last decade there has been considerable interest in a novel dynamical phenomenon of chimera states observed in an array of non-locally coupled oscillators where regions of coherence and incoherence coexist across the network. In this study we show how chimera states emerge in coupled logistic maps for certain specified initial conditions when the range and strength of coupling is varied. Here we show that these states are very robust and persist even in the presence of noise in the network parameters. On applying localized external perturbation to the incoherent regions, it is possible to obtain a completely coherent/incoherent dynamics in the whole network depending on the strength and sign of perturbation. This has important applications in the control of undesirable local dynamics, such as seizures in neural systems, or fibrillations in cardiac tissues.

**Keywords:** Chimera states, coupled logistic maps, control, pinning.

### **Introduction**

The coexistence of coherent and incoherent dynamics in an array of non-locally coupled, identical Ginzburg Landau oscillators was first observed by Kuramoto and Battogtokh [1]. Such a state was named “chimera” meaning, something composed of incongruous parts. Chimera states are defined as spatiotemporal patterns of synchrony and disorder in homogeneous, non-locally coupled excitable systems. Recently, this phenomenon has been experimentally demonstrated in a system of mechanical oscillators by Aaron *et al* [2]. What makes the chimera behavior interesting is the coexistence of distinct spatial regions of synchronized behavior and irregular incoherent behavior, in networks of identical and symmetrically coupled units. Such a phenomenon is also observed in nature in neuronal systems of birds and dolphins which sleep with half of their brain (synchronous state) while the other half remains awake (asynchronous state) [3].

Network topologies such as global (i.e. all-to-all) coupling and local (i.e. nearest-neighbor) coupling have been extensively studied. However, networks



with nonlocal coupling has been less studied in spite of applications in wide areas, *viz.*, chemical oscillators [4], excitable systems e.g., neural tissue [5], Josephson junctions [6], etc. There is now renewed interest in nonlocal networks with the recent discovery of chimera states [7]. In various numerical studies it has been shown that non-local coupling is a necessary condition for the occurrence of chimera states [8]; with local or global coupling, identical oscillators either synchronize or oscillate incoherently, but never do both simultaneously. In addition, the emergence of chimera states is extremely sensitive to the initial conditions and is observed only for carefully chosen initial conditions [9]. Numerous studies suggest that chimera states can exist in complex systems with nonlocal interactions. In this study we analyze the chimera states in nonlocally coupled logistic maps. Since it is unlikely that in any physical system, all the units are identical, the effect of heterogeneity on their collective behavior is of interest. With this objective we analyze the emergence and stability of chimera states in the presence of noise. In particular, we introduce noise in the initial conditions and in the system parameters, *viz.*, the bifurcation parameter and the coupling strength. In the event of undesirable dynamical behavior in localized regions, *viz.*, cardiac arrhythmia, epileptogenic neural activity, desynchronization in coupled chemical reactors, etc, there is a need to curb the incoherent dynamics in certain regions. With this objective we analyze the effect of external perturbation or pinning given selectively to regions of incoherence on the spatiotemporal dynamics of the whole system.

## 2 The Model and Simulations

### *Model:*

In this study we analyze the occurrence of chimera states in non-locally coupled logistic maps on one-dimensional lattice (with periodic boundary conditions). We consider identical logistic maps at every node of the lattice which are coupled to  $P$  neighbors on either side on the spatial lattice. The spatio-temporal dynamical system considered here is given by the equation

$$x_i^{t+1} = (1 - \varepsilon)f(x_i^t) + \frac{\varepsilon}{2P} \sum_{j=i-P}^{i+P} f(x_j^t) \quad (1)$$

where  $i = 1, 2, \dots, N$ ,  $t$  denotes the time step,  $\varepsilon$  the coupling strength and each node is coupled to  $P$  number of nodes on either side, i.e., a total of  $2P$  connections. The local function considered here is a logistic map given by  $f(x) = ax(1 - x)$ ,  $a$  being the bifurcation parameter. The radius of coupling  $r_c = P/N$  is a constant for all the nodes in the lattice. Since  $P = 1$  corresponds to local (nearest-neighbor) coupling and  $P = N/2$  corresponds to global coupling (all nodes connected to all other nodes),  $r_c$  lies between  $1/N$  and  $1/2$ . To mathematically quantify how spatially coherent or incoherent certain region in

the lattice is, the parameter  $R_i$  which gives the *degree of coherence* in a local region surrounding the node  $i$  is defined as

$$R_i = \lim_{N \rightarrow \infty} \frac{1}{2\delta} \left| \sum_{|j-i| \leq \delta} e^{i\psi_j} \right| \quad (2)$$

where  $i = 1, 2, \dots, N$ ,  $\psi_j = \sin^{-1}(2x_j - \max_k x_k - \min_k x_k)$ ,  $\delta$  denotes the neighborhood of a node on either side for which the extent of coherence is measured,  $\max_k x_k$  and  $\min_k x_k$  denote the maximum and minimum values of  $x_k$  respectively, where  $k$  is a node in the neighborhood of node  $j$ .  $R_i$  measures the degree of coherence in an interval defined by  $\delta$ , in that as  $N \rightarrow \infty$  and  $\delta \rightarrow 0$ ,  $R_i \rightarrow 1$  in the coherent interval and  $0 < R_i < 1$  in the incoherent interval. In Figure 1(a) is shown the spatial dynamics of  $x$  at a given time  $t$ , after eliminating the transients. In Figure 1(b) is shown the spatial behavior of  $R$  for  $\delta = 10$ . It may be noted that the value of  $R$  in the coherent region is close to 1 in Figure 1(b) ( $\delta = 10$ ). In the incoherent regions, the value of  $R$  is lower than in the coherent regions. Thus, analyzing the behavior of  $R_i$  helps in detecting the presence of chimera states in the lattice.

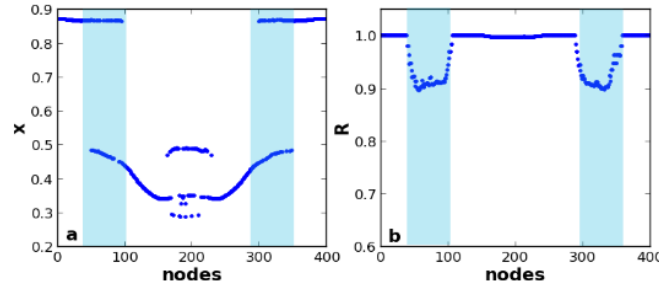


Fig. 1: a) Spatial dynamics of  $x$ , b) spatial dynamics of  $R$  for  $\delta = 10$ . The system size  $N = 400$ , and the system parameters are  $a = 3.8$ ,  $r_c = 0.32$ ,  $\varepsilon = 0.24$ . Regions shaded in blue are the regions of incoherence.  $\delta = 10$  is used for all the succeeding  $R$  calculations.

### Initial Conditions:

In numerous studies it has been shown that the emergence of chimera states is extremely dependent on the initial conditions. Here we consider three different initial distributions of  $x$  to induce chimera states in the 1d spatially coupled lattice.

**TYPE I:** In this case, the distribution of  $x$  in the initial state is set to be the same in certain regions of the lattice, and randomly distributed between an interval in small intervals between them as defined below and depicted in Figure 2(a) [1]:

$$i \in [0, N/8) \text{ and } [7N/8, N), x_i(0) = 0.45$$

$$i \in [N/4, 3N/4), x_i(0) = 0.9$$

$$i \in [N/8, N/4) \text{ and } [3N/4, 7N/8), x_i(0) \in I, I = [0.4, 0.5] \cup [0.85, 0.95]$$

After eliminating the transients we observe the emergence of chimera states in the lattice: the coherent regions are interspersed between the incoherent regions interspersed in between them as seen in Figure 2(d). The spatial behavior of  $R$  in Figure 2(g) further confirms the chimera state.

**TYPE II:** A half compressed  $\tanh$  function in the first half of the lattice and its mirror image in the second half as shown in Figure 2(b) is considered and is given by

$$i \in [0, N/2), x_i(0) = \frac{1}{2} \left( \tanh \left( \frac{3(i - N/4)}{N/4} \right) + 1 \right)$$

$$i \in [N/2, N), x_i(0) = \frac{1}{2} \left( \tanh \left( \frac{3(3N/4 - i)}{N/4} \right) + 1 \right)$$

The chimera behavior is observed in this case also as shown in Figure 2(e) and 2(h), very similar to that observed with type I initial conditions, except that the incoherent intervals are not so well defined.

**TYPE III:** In this case the initial distribution of  $x$  is considered to be a sine function over the lattice given by

$$i \in [0, N), \text{init } x_i = \sin(i\pi/N)$$

as shown in Figure 2(c). The spatial behavior of  $x$  in Figure 2(f) and  $R_i$  in Figure 2(i) exhibits emergence of chimera states. Unlike type I and type II conditions, in this case there is neither a sharp discontinuity in the  $x$  value along the lattice, nor a flat region with nodes having the same  $x$  value. As can be seen in figures 2(f) and 2(i), the spatial dynamics of  $x$  and  $R$  is shifted when compared to the dynamics with type I and type II initial conditions (shown in figures 2(d), (e), (g), (h)). In the case of type II or type III initial conditions, the chimera states are observed only when the local dynamics is chaotic, while the type I initial conditions give rise to chimera states even when the local dynamics is periodic; in this case the regions of incoherence are spatially and temporally periodic while the coherent regions are spatially synchronous. Thus we observe that different types of initial conditions can give rise to chimera states, as long as the coupling is non-local.

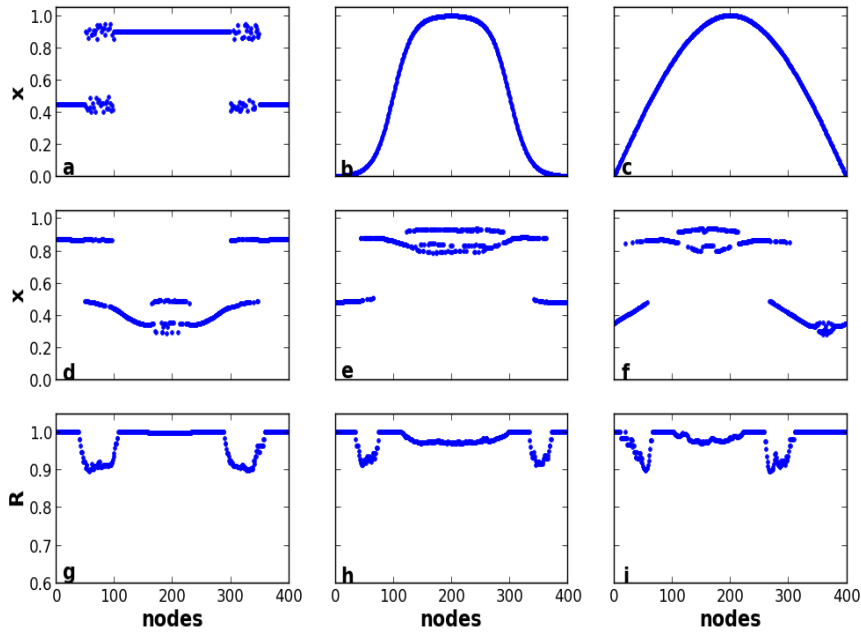


Fig. 2: The three types of initial conditions considered here, *viz.*, type I, II and III, are shown in (a) – (c) and in (d) – (f) the spatial dynamics of non-locally coupled logistic maps obtained after eliminating 50000 transients for the corresponding initial conditions is depicted. Figures (g) – (i) depicts the spatial dynamics of  $R$  corresponding to the dynamics of  $x$  in (d) – (f) respectively. The parameters  $(r_c, \varepsilon)$  for the plots (d), (g) are (0.32, 0.24), (e), (h) are (0.24, 0.24) and (f), (i) are (0.24, 0.24).

**Sensitivity to initial conditions:**

In order to see the dependence on the initial conditions for the emergence of chimera states, in Figure 3 we show the spatio-temporal dynamics of the system after eliminating 50000 transients for the parameters chosen in the chaotic regime. In Figure 3(a) is shown the dynamical state attained on using type I initial conditions (defined above) and in Figure 3(b) dynamical state attained on using random initial, *i.e.*  $x_i(0)$  is a random number in the range (0,1). It may be noted that in Figure 3(a) with type I initial conditions, the system exhibits regions of incoherence interspersed between regions of coherence, while no such dynamical behavior is observed with random initial conditions (Figure 3(b)), for same set of parameter values. The spatio-temporal dynamics of the lattice was analyzed for 50 different random initial configurations and chimera behaviour was not observed in any of these cases. Thus we may conclude that though the emergence of chimera behaviour is sensitive to initial conditions.

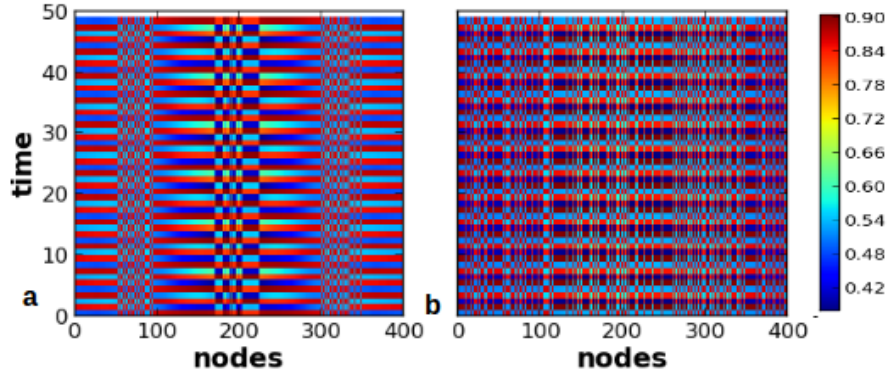


Fig. 3: Spatio-temporal dynamics of the non-locally coupled logistic maps with (a) type I initial conditions, (b) random initial conditions in the interval  $(0, 1)$  for  $a = 3.8$ ,  $r_c = 0.32$  and  $\varepsilon = 0.24$ .

### 3 Results and Discussions:

#### Analysis of $r_c - \varepsilon$ parameter space:

The emergence of chimera states is observed to be dependent on two parameters, *viz.*, the range of coupling,  $r_c$  and the strength of coupling,  $\varepsilon$ . In Figure 4 is shown the  $r_c - \varepsilon$  parameter-space plot indicating various dynamics observed in one-dimensional non-locally coupled logistic maps for type I initial conditions. The chimera behavior is observed for a wide range of coupling shown by regions in blue when the coupling strength  $\varepsilon$  is low and  $K$  denotes the wave number of the spatial dynamics. It is observed that for a given coupling strength, chimera states with higher wave numbers occur at lower radius of coupling than those with lower wave numbers. Also, with increase in the range of coupling  $r_c$ , the chimera behavior is observed even for very lower coupling strengths,  $\varepsilon$ . The red and green regions correspond to temporally periodic dynamics with period  $p = 4$  and  $2$  respectively. The yellow region corresponds to chimera dynamics with  $p = 4$ , while the purple region indicates chimera dynamics with  $p = 2$ .

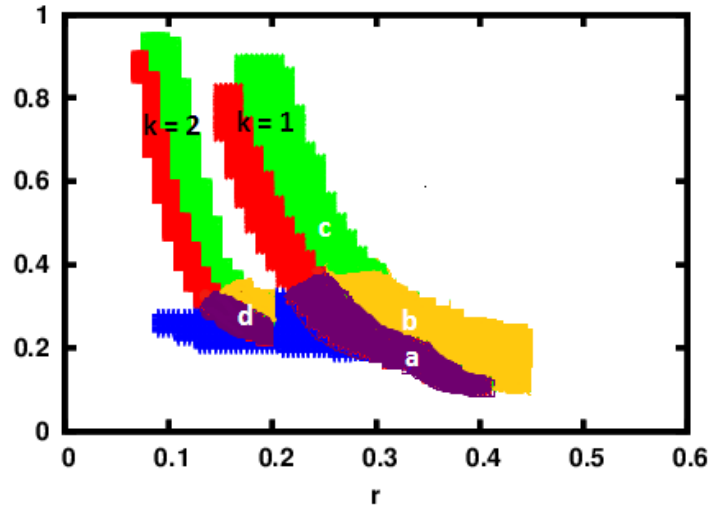


Fig. 4:  $r_c - \varepsilon$  parameter-space plot shown for non-locally coupled logistic maps with  $N = 400$  with type I initial conditions. The values of  $a$  is 3.8. The chimera states emerge in regions shown in blue, purple and yellow, while red and green regions correspond to temporal periodic dynamics with period-4 and period-2 respectively. The yellow region indicates intersection of blue and green regions and purple region, the intersection of blue and red regions.  $K$  denotes the wave number of the spatial dynamics.

In Figure 5 the spatiotemporal dynamical behavior of the system at points marked 'a', 'b', 'c', and 'd' in Figure 4 is depicted in the third column. It may be noted from the spatio-temporal dynamics of  $x$  corresponding to point 'a' and 'b' that as the coupling strength  $\varepsilon$  increases from 0.2 to 0.24, the degree of coherence increases (for fixed  $r_c = 0.32$ ). On further increasing the coupling strength ( $\varepsilon > 0.3$ ), the regions of incoherence disappear and the lattice is seen to exhibit coherent dynamics (results not shown). The spatio-temporal dynamics at larger coupling strength,  $\varepsilon = 0.42$  ( $r_c = 0.24$ ) corresponding to 'c' is mainly coherent. The spatio-temporal dynamics corresponding to point 'd' exhibits higher wave number ( $K = 2$ ) and period ( $p = 4$ ).

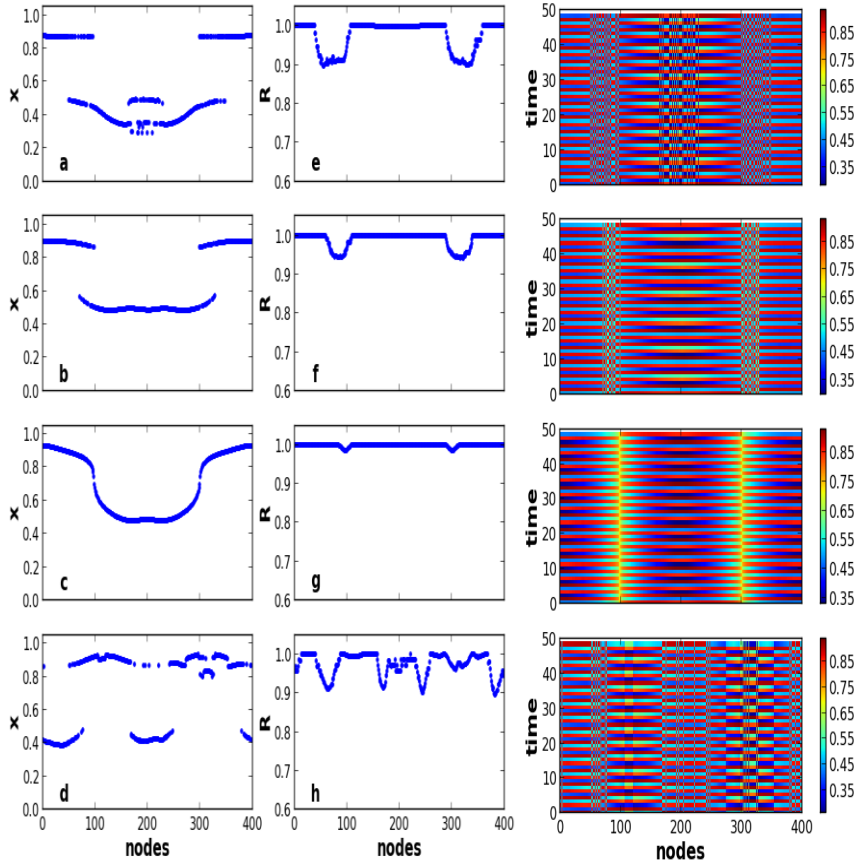


Fig. 5: (a) - (d) depicts the spatial dynamics ( $x_i$  vs  $i$ ) at points a, b, c and d respectively in the  $r_c - \varepsilon$  parameter-space plot (Figure 4). (e) – (h) spatial plots of  $R_i$  vs  $i$  corresponding to the plots (a) – (d). The parameter values ( $r_c, \varepsilon$ ) for the points ‘a’, ‘b’, ‘c’, and ‘d’ in Figure 4 correspond to (0.32,0.2), (0.32, 0.24), (0.28,0.42) and (0.15, 0.24) respectively. The points ‘a’, ‘b’, and ‘c’ corresponds to wave number  $K = 1$ , while point ‘d’ to wave number  $K = 2$ . The spatiotemporal dynamics is shown in the third column. For the calculation of  $R_i$ .

Thus we observe that for fixed coupling strength  $\varepsilon$ , the incoherence in the spatial dynamics decreases with an increase in the radius of coupling. This is confirmed from the spatial behavior of degree of coherence,  $R_i$ , for different values of radius of coupling in Figure 6(a). Similarly, for weak coupling the dynamics is incoherent, but as the coupling strength is increased through a critical value (for fixed radius of coupling), coherence emerges and on further increase in the coupling strength, complete synchronization is observed. This is quantified in terms of  $R_i$  in Figure 6(b).



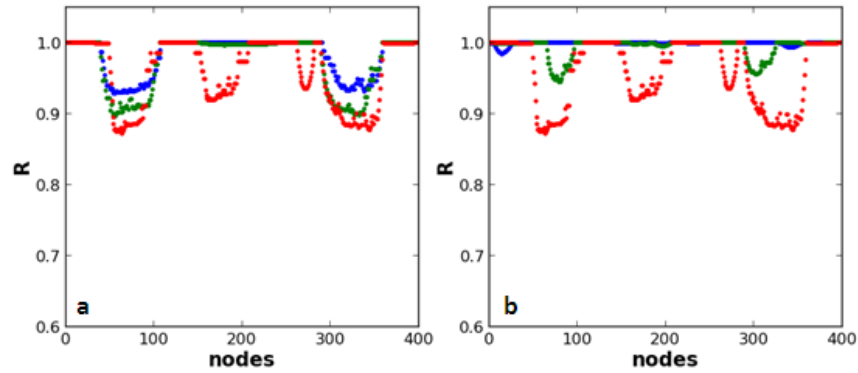


Fig. 6: (a) Spatial behavior of  $R$  is shown for various values of radius of coupling,  $r_c$ : 0.2 (red), 0.32 (green) and 0.4 (blue) for a constant coupling strength,  $\varepsilon = 0.24$ . There is a clear decrease in the spatial incoherence with increase in the value of  $r_c$ . (b) Spatial behavior of  $R$  is shown for various values of coupling strength,  $\varepsilon$ : 0.24 (red), 0.32 (green) and 0.36 (blue) for a constant,  $r_c = 0.2$ . We see a clear decrease in the degree of spatial incoherence with increase in the value of  $\varepsilon$ . The remaining parameters for figures 6(a),(b) are  $a = 3.8$ ,  $N = 400$ .

#### ***Robustness of chimera states to perturbations :***

In real practical situations, it is unlikely to have the same system parameters over the entire spatial domain, e.g., the junctional coupling strengths,  $\varepsilon$  may vary between cells in a neural tissue, or the growth parameter  $a$  may not be same in all subpopulation patches, etc. To mimic such a scenario, we introduce small random variations in the system parameters  $a$  and  $\varepsilon$ , i.e.,  $a \pm \delta a_i$  and  $\varepsilon + \delta \varepsilon_i$ . Since the occurrence of chimera states is sensitive to the initial conditions, we also introduce noise in the initial conditions, i.e.,  $x_i(0) \pm \delta x_i(0)$  ( $x_i(0)$  refers to type I initial conditions), and analyze the emergence and stability of the chimera states in such a heterogeneous coupled logistic maps. In Figure 7(a)-(d) is shown the spatial dynamics of  $x$  and in the adjacent plots (2<sup>nd</sup> panel) the spatio-temporal dynamics for varying coupling strengths. It is observed that at lower coupling strengths, the lattice exhibits incoherent dynamics in the presence of noise. As the coupling strength is increased, incoherence in the dynamics is reduced and emergence of chimera states is clearly observed for intermediate coupling strengths ( $0.24 < 0.35$ ). For  $\varepsilon > 0.35$ , the lattice exhibits spatially coherent dynamics.

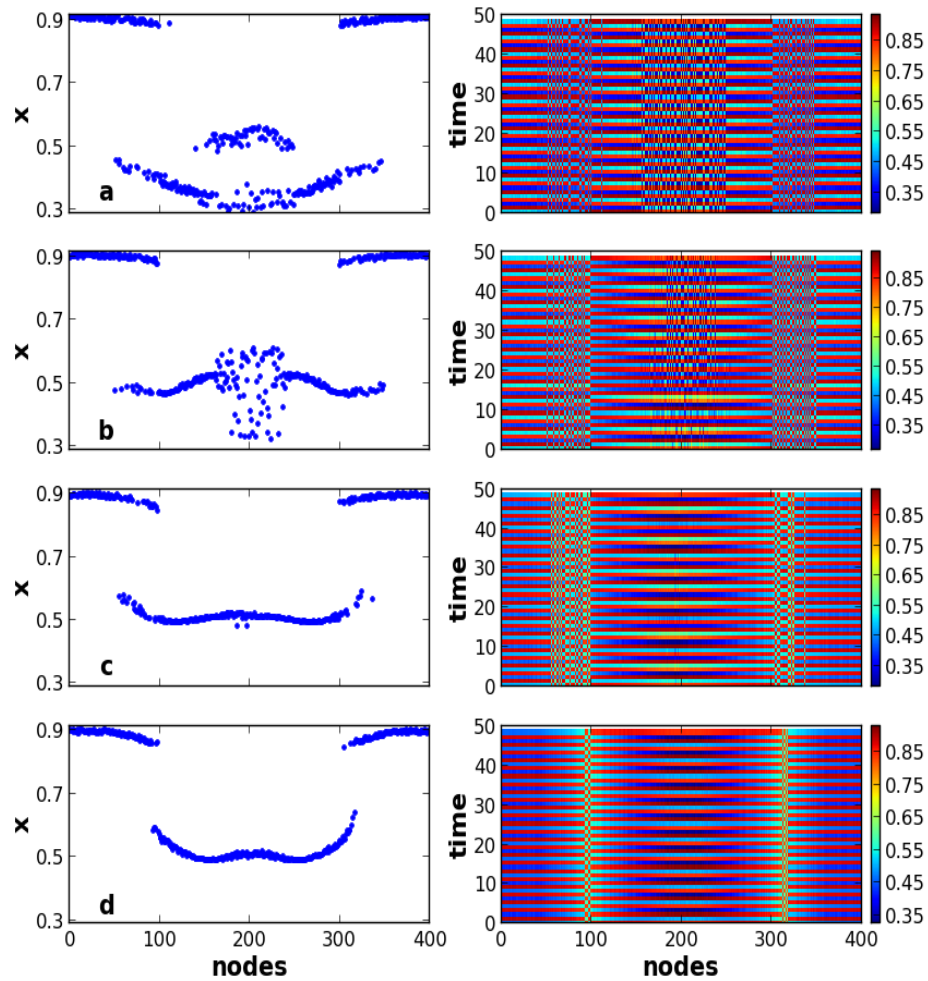


Fig. 7: In (a) – (d) is shown the spatial dynamics of  $x$  and their corresponding spatio-temporal plots (in the 2<sup>nd</sup> column) for different coupling strengths,  $\varepsilon = 0.2, 0.24, 0.3$  and  $0.35$  respectively with a variation of  $\pm 0.005$ . The parameters values of the lattice are  $a = 3.8 \pm 0.04$ , and the random variations to the type I initial conditions as  $\pm 0.05$ .

### ***Effect of External Perturbation on the Chimera States:***

In various physical and biological systems such as power grids or excitable tissues (e.g., cardiac or neuronal tissues), the synchronous movement of all their parts is extremely crucial for their proper functioning [10]. Localized regions of incoherence in such systems may cause hindrance to their performance and in extreme situations may even completely destabilize the system [11]. In such situations, there is clearly a need to address local disturbances/incoherent

dynamics and bring the system back to its original synchronous dynamical state. Here we attempt to analyze the effect of applying localized external perturbation or “pinning” to the incoherent regions and see if the system is driven to spatially synchronous state or the whole lattice exhibits incoherent dynamics. The objective is to manipulate the dynamics in the event of the system exhibiting undesired local dynamics. For example, extended periods of synchronization in the brain, results in epileptic seizures and there exists need for external intervention. In diffusively coupled logistic maps, it has been shown by Parekh *et al* [12] that negative pinning suppresses chaos while positive pinning induces/enhances chaos. In Figure 8(a), we observe that on applying negative pinning to the incoherent regions, the degree of incoherence is reduced and can be completely suppressed, while applying positive pinning as shown in Figure 8(b), the degree of incoherence is enhanced. However, it may be noted that the coherent dynamics attained by selectively pinning the regions of incoherence exists only as long as the pinning is being given. In Figure 9 is shown the effect of removing the external pinning after having applied for a certain period of time. Initially the system is considered to be exhibiting chimera behavior when no pinning is applied to (blue). The region of incoherence is decreased both in the spatial spread and extent on applying negative pinning selectively to the nodes in the incoherent region (red). On switching off the external pinning and eliminating transients, we observe that the system goes back to the original dynamical state and exhibits spatial incoherence regions which are much narrower than the initial case, i.e., on switching off the external perturbation, the extent of spread of the incoherent dynamics is reduced, but not completely eliminated.

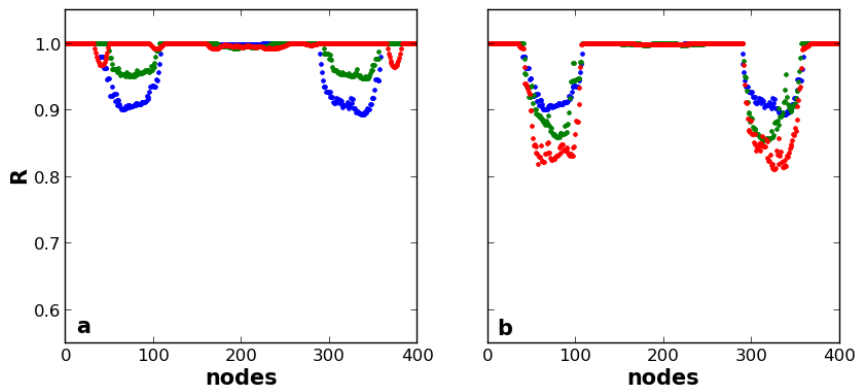


Fig. 8: (a) Spatial behavior of  $R$  for the parameters  $N = 400$ ,  $r_c = 0.32$ ,  $\varepsilon = 0.24$ , shown on selectively pinning the incoherent regions with varying strengths of (a) negative pinning: -0.05 (green) and -0.15 (red); (b) positive pinning: 0.03 (green), 0.08 (red). The plots in blue correspond to “no pinning” in both (a) and

(b). It is clear that negative pinning suppresses while positive pinning enhances incoherence.

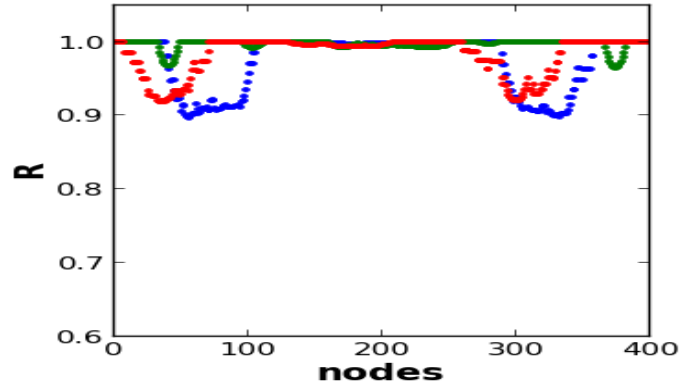


Fig. 9: Spatial behavior of  $R$ : i) no pinning (blue), ii) selective pinning of  $-0.13$  (green) after eliminating 50000 transients and iii) eliminating 50000 transients after removing the selective pinning (red). Here,  $a = 3.8$ ,  $N = 100$ ,  $r_c = 0.32$ ,  $\varepsilon = 0.18$ .

## Conclusions

In this study we carried out a systematic analysis for the emergence and stability of chimera behavior in non-locally coupled logistic maps. We discuss the emergence and disappearance of chimera states as a function of the radius and strength of coupling. The chimera states are observed to be robust to small random variations in the initial conditions and system parameters for reasonable strength and radius of coupling. We also showed that it is possible to suppress/induce incoherence in spatially localized regions as this may be desirable in certain situations such as epileptic seizures, or cardiac fibrillation. However, the persistence of pinning is required for achieving the desired behavior. This has important applications in many complex physical and biological systems.

## References

1. Kuramoto and Battogtokh, *Complex Systems* **5**(4), 380 (2002).
2. Aaron M. Hagerstrom, Thomas E. Murphy, Rajarshi Roy, Phillip Hovel, Iryna Omelchenko, Eckehard Scholl, *Nature Physics* **8**(9), 658 (2012).
3. C. G. Mathews, J. A. Lesku, S. L. Lima, C. J. Amlaner, *Ethology* **112**(3), 286 (2006).
4. A. S. Mikhailov and K. Showalter, *Phys. Rep.* **425**(2), 79 (2006).

5. R. Vicente, L. L. Gollo, C. R. Mirasso, I. Fischer, and P. Gordon, *National Academy of Sciences, Proceedings* **105**(44), 17157 (2008)
6. K. Wiesenfeld, P. Colet, and S. H. Strogatz, *Phys. Rev. Lett.*, **76**(3), 404 (1996).
7. O. E. Omel'chenko, M. Wolfrum, and Y. L. Maistrenko, *Phys. Rev. E*, **81**(6), 065201 (2010).
8. Daniel M Abrams, Steven H Strogatz, *Chaos*, **16**(6), 21 (2006).
9. Iryna Omelchenko, Yuri Maitsrenko, Philipp Hovel, Eckehard Scholl, *Phys. Rev Lett.*, **106**(23), 234102 (2011).
10. Martin Rohden, Andreas Sorge, Marc Timme, Dirk Witthaut, *Phys. Rev. Lett.*, **109**(6), 064101 (2012).
11. Erik A Martens, Shashi Thutupalli, Antoinne Fourriere, Oskar Hallatschek, *National Academy of Sciences, Proceedings*, **Vol. 110**(26), 10563 (2013).
12. Nita Parekh, S. Parthasarathy, Somdatta Sinha, *Phys. Rev. Lett.* **81**(7),. 1401 (1998).